

# Heavy metal removal using alkali activated kaolinite in the $\text{CaO-Al}_2\text{O}_3\text{-SiO}_2\text{-H}_2\text{O}$ system

## Abstract

The transformation of kaolinite was examined at 175°C for 24 h in the CaO-Al<sub>2</sub>O<sub>3</sub>-SiO<sub>2</sub>-H<sub>2</sub>O (CASH) system, which is important in cement science and especially in, cement chemistry and is closely related to the pozzolanic reaction, the CaO-aggregate reaction and the glass fibre reinforcement of hardened cement. The hydration products were characterized by X-ray diffraction, scanning electron microscopy, Fourier transformed infrared spectroscopy, Magic Angle Spinning Nuclear Magnetic Resonance and thermogravimetric analysis in order to elucidate their mineral chemistry and microstructure. Results reveal that several poorly crystalline phases were formed, with un-reacted Ca(OH)<sub>2</sub> appearing at shorter reaction times. Hydrogarnet tends to form more rapidly than tobermorite. It was transformed into aluminium-substituted tobermorite with curing time. A batch experimental study confirmed that kaolinite-based calcium silicate hydrates are effective for the treatment of acid mine drainage, particularly in removing metal ions and ammonium.

**Keywords:** kaolinite, cash system, cement, calcium silicate hydrates, hydrogarnet, tobermorite

Volume 1 Issue 4 - 2017

 Carlos A Ríos,<sup>1,2</sup> Craig D Williams,<sup>2</sup> Michael A Fullen<sup>2</sup>
<sup>1</sup>Industrial University of Santander, Colombia

<sup>2</sup>The University of Wolverhampton, UK

**Correspondence:** Carlos A Ríos, Industrial University of Santander, Colombia, Fax 01902 322714, Email C.A.RiosReyes@wlv.ac.uk

**Received:** June 17, 2017 | **Published:** November 30, 2017

## Introduction

Most of calcium silicate hydrate or calcium aluminosilicate hydrate, CS(A)H, and related phases are relevant to Cement industry and have potential as geothermal well sealants as well as autoclaved construction materials. The CS(A)H system is highly complex and is comprised of crystalline to amorphous phases with variable composition that build up a wide family of phases, which are interesting for the variety of their structural arrangements, the peculiarity of the transformation processes in which they are involved and the relationships with compounds which form during the hydration of the Portland cement.<sup>1</sup> Different studies have been carried out on the hydrothermal transformation of kaolinite or metakaolinite into CS(A)H phases, with particular attention on tobermorite. The most widely studied aluminium-bearing materials and their effects on various aspects of tobermorite formation include:  $\gamma\text{-Al}_2\text{O}_3$ , Al(OH)<sub>3</sub>, kaolinite, metakaolinite, zeolite and solid waste materials. The raw materials used in the synthesis of tobermorite usually contain aluminium-bearing impurities and therefore the role of aluminium in the stabilization of tobermorite has been reported in several studies.<sup>2-10</sup> A chronology of the main results from these studies is presented as follows.<sup>11-12</sup> undertook a microstructural study on autoclaved clinker and slag-lime pastes in the presence and absence of silica sand using scanning electron microscopy, determining the formation of several hydration products, such as C-S-H, hydrogarnet and tobermorite. The formation of hydrogarnet for ratios of Al/(Si + Al) in the range of 0.12–0.50 when kaolinite is used as the source of aluminium was reported by.<sup>13</sup> Mitsuda<sup>3</sup> studied the effect of substitution of Si by Al in tobermorite formed in the CaO-SiO<sub>2</sub>-H<sub>2</sub>O system. Van Aardt<sup>14</sup> investigated the reaction between Ca(OH)<sub>2</sub> and minerals containing alumina, which forms C<sub>4</sub>A-hydrates and/or hydrogarnet (calcium-alumina-silicate hydrate), depending on temperature. Serry et al.<sup>15</sup> studied metakaolin-lime hydration products, determining that gehlenite hydrate (C<sub>2</sub>ASH<sub>8</sub>) was the main hydration product and its amount increased with reaction time, whereas hydrogarnet crystallized at the early stages of

hydration in the low-lime content mixtures, increasing with curing time. Atkins et al.<sup>16</sup> studied the solubility properties of ternary and quaternary compounds in the CaO-Al<sub>2</sub>O<sub>3</sub>-SO<sub>3</sub>-H<sub>2</sub>O system, with ettringite (C<sub>6</sub>A<sub>3</sub>H<sub>32</sub>) and hydrogarnet (C<sub>3</sub>AH<sub>6</sub>) dissolving congruently, whereas monosulphate (C<sub>4</sub>AH<sub>2</sub>) and tetra-calcium aluminat hydrate (C<sub>4</sub>AH<sub>13</sub>) dissolved incongruently. The reaction mechanism of the hydrothermally treated CaO-SiO<sub>2</sub>-Al<sub>2</sub>O<sub>3</sub> and CaO-SiO<sub>2</sub>-Al<sub>2</sub>O<sub>3</sub>-CaSO<sub>4</sub> systems was conducted by Al-Wakeel & El-Korashy,<sup>17</sup> using mixtures of CaO, amorphous SiO<sub>2</sub> and kaolinite in the presence or absence of SO<sub>4</sub><sup>2-</sup> ions (added as CaSO<sub>4</sub>·2H<sub>2</sub>O), which were treated in suspension under hydrothermal conditions at temperatures of 80-200°C. The results indicate the occurrence of several C-S-H phases, which are then transformed into Al-substituted 11Å tobermorite. In both systems excess Al<sub>2</sub>O<sub>3</sub> appeared as a hydrogarnet phase.<sup>18</sup> First reported the occurrence of hydrogarnet-type cubic crystals in polymer-modified mortars.<sup>19</sup> investigated the hydrothermal conversion of kaolinite with calcium hydroxide and dissolution of reaction products in hydrochloric acid, obtaining different reaction products, such as hibschtite, omisteinbergite, tobermorite and jaffeite. Klimesch and Ray investigated the effects of quartz particle size on hydrogarnet formation and the nature of hydration products in unstirred autoclaved metakaolin-lime-quartz<sup>20-22</sup> and kaolin-lime-quartz<sup>23</sup> slurries. Hydrogarnet was always among the first phases formed and invariably appeared before 11Å tobermorite and with increasing reaction time the amount of hydrogarnet decreased and finally disappeared, while Al-substituted 11Å tobermorite increased concurrently, and the continued existence of hydrogarnet depended on such factors as reaction time and initial Al<sub>2</sub>O<sub>3</sub> content in the raw mixture.<sup>23</sup> Klimesch et al.<sup>22</sup> monitored the evolution of hydration products in unstirred autoclaved metakaolin-lime-quartz slurries with reaction time using thermogravimetric analysis, concluding that hydrogarnet was always one of the first phases formed at all metakaolin additions and invariably appeared before tobermorite. Frias et al.<sup>24</sup> studied the effect of curing temperature on the reaction kinetics of a metakaolin/lime mixture, determining from thermal analysis (TG and DTA) data

different appearance sequence of the hydrated phases. Coleman et al.<sup>25</sup> investigated the synthesis of hydrogarnet and tobermorite from newsprint recycling residue. A batch sorption study confirmed that the as-synthesized tobermorite was effective in removing  $\text{Cd}^{2+}$ ,  $\text{Pb}^{2+}$  and  $\text{Zn}^{2+}$  from acid aqueous media. Frías et al.<sup>26</sup> evaluated the effect of different parameters on the reaction kinetics in metakaolin/lime and metakaolin-blended cement matrices at 60°C, defining different sequences of formation of the hydrated phases according to the matrix. Siauciunas et al.<sup>27</sup> studied the influence of  $\text{SiO}_2$  modification on the formation and stability of hydrogarnet and Al-substituted 11Å tobermorite during hydrothermal synthesis, determining that hydrogarnet always tended to form more rapidly than tobermorite, although with increasing reaction time hydrogarnet started to fracture and its amount decreased. Frías et al.<sup>28</sup> investigated the influence of metastable hydrated phases like C-S-H,  $\text{C}_2\text{ASH}_8$  and  $\text{C}_4\text{AH}_{13}$  on the pore size distribution and degree of hydration of metakaolin-blended cements cured at 60°C. According to them, these phases are stable at room temperature, but some ( $\text{C}_2\text{ASH}_8$  and  $\text{C}_4\text{AH}_{13}$ ) are metastable phases, converting to hydrogarnet for long curing times at elevated temperatures.<sup>29</sup> Conducted a selective synthesis of phillipsite and hydrogarnet, employing  $\text{Ca}(\text{OH})_2$  under mild chemical conditions, provided a potential alternative for the recycling of fly ash and investigated the heavy metal cation removal abilities towards lead ions of the synthetic phillipsite.<sup>30</sup> Carried out XAS experiments using synchrotron radiation and concluded that the hydration of  $\text{C}_4\text{AF}$  forms hydrogarnet in which Fe randomly substitutes for Al as well as an amorphous  $\text{FeOOH}$  phase, intermediate products like  $\text{AF}_m$  (ettringite) are also formed but rapidly evolve to hydrogarnet, iron does not seem to be incorporated in the  $\text{AF}_m$  structure. Therefore, the efficiency of the C-S-H materials in removing heavy metals should be considered.<sup>31</sup> studied phase and microstructure evolution during hydrothermal solidification of clay-quartz mixture using marble as a lime source, with tobermorite and hydrogarnet being the major phases formed after reaction, which are responsible for strength development in the as-synthesized materials suitable for building.<sup>32</sup> studied the effect of curing temperature on reaction kinetics in a metakaolin/lime mixture cured at 60°C and after 60 months of hydration, evaluating the stabilities of hydrated phases formed during the pozzolanic reaction. The results obtained by this author show that metastable hexagonal phases ( $\text{C}_2\text{ASH}_8$  and probably  $\text{C}_4\text{AH}_{13}$ ) coexist with a stable cubic phase (hydrogarnet) in the absence of lime.<sup>33</sup> Carried out a study on solid-state  $^{29}\text{Si}$  and  $^{27}\text{Al}$  NMR on Si-substituted hydrogarnet. The appropriate combination of NMR and Rietveld analyses of the X-ray and neutron diffraction patterns allowed better understanding of the formation of  $\text{Ca}_3\text{Al}_2(\text{SiO}_4)_{3-x}(\text{OH})_{4x}$  hydrates during the hydration of  $\text{Ca}_3\text{Al}_2\text{O}_6$  in the presence of nanospheres of amorphous silica.<sup>34</sup> used  $^{29}\text{Si}$  NMR and  $^{27}\text{Al}$  MAS NMR spectroscopy to study autoclaved cement-quartz pastes containing 0-30.5% metakaolin as either quartz or cement replacement.

These aspects are very important from the point of view of the engineering and microstructural properties, which could have associated a negative effect on the performance of the as-synthesized products. The technological interest of tobermorite arose from its role as the primary binder of most autoclaved calcium silicate based building materials. However, more recently the ion exchange characteristics of synthetic 11Å tobermorite and its aluminium-substituted analogue have been investigated with respect to their potential in nuclear and hazardous wastewater conditioning.<sup>35-40</sup>

The objective of the study is to investigate the chemical

transformation of kaolinite under hydrothermal conditions at 175°C for 24h and establish the reaction sequence and nature of the C-S-H phases formed. In addition, this study examines at laboratory-scale the effectiveness of kaolinite-based calcium silicates as sorbents in removing metal ions and ammonium from acid mine drainage (AMD), which could be used as environmentally friendly materials with high remediation abilities.

## Experimental procedures

### Materials

In the present study, kaolinite (Supreme Powder, ECC International, UK) or metakaolinite were used as starting materials. Kaolinite (composition 46.44%  $\text{SiO}_2$ , 38.80%  $\text{Al}_2\text{O}_3$ , 0.03%  $\text{TiO}_2$ , 0.52%  $\text{Fe}_2\text{O}_3$ , 0.08%  $\text{MgO}$ , 0.33%  $\text{Na}_2\text{O}$  and 0.69%  $\text{K}_2\text{O}$ ) was used without further purification. Metakaolinite has extraordinarily high pozzolan reactivity and it was prepared by calcining kaolinite at 600°C in air for 2h. All solid starting materials were first ground and particles <75µm selected by sieving, before gels were prepared. Activator reagents included  $\text{CaCO}_3$  (Griffic),  $\text{Al}(\text{OH})_3$  (Fisher Scientific International Company), precipitated  $\text{SiO}_2$  (BDH), and distilled water using standard purification methods. A sample of acid mine drainage collected from the abandoned copper-lead-zinc deposit at Parys Mountain (North Wales) was used as a natural solution in a batch experiment.

### Synthesis of C-S-H phases

The method used in this study was based on that of Kalousek.<sup>13</sup> The starting material was the following mixture:  $\text{CaO}$ +kaolinite, identified as KAOAd. Starting mixtures were prepared with molar compositions of  $\text{Al}/(\text{Si} + \text{Al})$  and  $\text{Ca}/(\text{Si} + \text{Al})=0.10-0.13$  and 6.50-1.00. To activate the raw materials with calcium oxide solutions to synthesize hydrated calcium silicates, reagent-grade calcium carbonate ( $\text{CaCO}_3$ ) was calcined at 1000°C for 1h to obtain  $\text{CaO}$ . For comparison, a reaction gel was prepared using the following pure chemical reagents: amorphous  $\text{Al}_2\text{O}_3$  (prepared by calcination of  $\text{Al}(\text{OH})_3$  at 550°C for 1h), precipitated  $\text{SiO}_2$ ,  $\text{CaO}$  and distilled water. The resulting mixtures were transferred to 20cm<sup>3</sup> PTFE-lined stainless steel autoclaves and the hydrothermal synthesis was performed under static conditions using water/solid ratios of 1.50-2.28 at 175°C for different curing times. On removal from the oven they were quenched in cold water and the product recovered by vacuum filtration using a filter funnel and Whatman paper to remove excess water. Once the water was extracted from the filtered product, the sample was rinsed with ethanol ( $\text{C}_2\text{H}_5\text{OH}$ ) and dried at 80°C overnight. Further details of the gel compositions and synthesis conditions.

### Characterization of calcium silicate hydrates

The synthesis phase(s) in the solids products were identified by powder X-ray diffraction (XRD), performed on a Philips PW1710 diffractometer equipped with  $\text{Cu-K}\alpha$  radiation (40kV and 40mA) and theta compensating divergence slits. Data were collected in 45min over the  $2\theta$  range 3-50°, with a step size of 0.02° with phase identification being made by searching the ICDD powder diffraction file database. Surface morphology was investigated using a Zeiss EVO 50 scanning electron microscope equipped with secondary detector and EDX on gold-coated samples. Fourier transform infrared (FT-IR) spectra were recorded in the range 400-4000cm<sup>-1</sup> on a Mattson Genesis II FT-IR spectrometer. However, we discuss only the 1200-400cm<sup>-1</sup> region,

because this is where the spectra show remarkable changes. MAS NMR spectra for  $^{29}\text{Si}$  and  $^{27}\text{Al}$ , respectively, were recorded at room temperature on a Varian Unity Inova spectrometer under the following analytical conditions: MAS probe 7.5 and 4.0mm; frequency 59.6 and 78.1MHz; spectral width 29996.3 and 100000.0Hz; acquisition time 30 and 10 $\mu\text{s}$ ; recycle time 120 and 0.5sec; number of repetitions 15 and 2200; spinning rate 5040 and 14000Hz; pulse angle (DP) 90.0 and 18.9°. The chemical shifts were referenced to tetramethylsilane (TMS) for  $^{29}\text{Si}$  and 1M  $\text{AlCl}_3$  aqueous solution for  $^{27}\text{Al}$ . The  $^{29}\text{Si}$  chemical shift of the peaks were analysed using the  $\text{Q}^n(\text{mAl})$  classification, with the Si tetrahedron is connected to mAl and (n-m) Si tetrahedral where  $n=0$  to 4 and  $m=0$  to n. Thermogravimetry was performed on a Mettler Toledo TG50 thermobalance in the temperature range of 25–700°C, with a heating rate of 10°C  $\text{min}^{-1}$  under flowing air. Mass losses were determined by employing both TGA and DTG curves. The second derivative differential thermal curve was used for peak temperature determinations.

### Batch experiment and water analyses

In order to investigate the efficiency of selected kaolinite-based calcium silicate hydrates for removing metal ions and ammonium from AMD, a laboratory batch experiment was conducted at room temperature. A weighed amount of sorbent (0.25g) was introduced in PVC plastic bottles of 100ml, then a volume of 20ml of AMD with  $\text{pH}=1.96$  was added. Later, the sorbents and AMD were mixed by continuous shaking during 30minutes. At the scheduled reaction time the bottles were removed from the shaker and the adsorbents were separated by filtration, while filtrates were stored at 4°C in a refrigerator for chemical analyses. All measurements were performed according to the Standard Methods for the Examination of Water and Wastewater. The pH and electrical conductivity of the raw AMD and the filtrates obtained after batch experiments were measured using a pH 211 Auto-calibration bench pH/mV meter (Hanna instruments) and a Cond 315i conductivity meter (WTW instruments), respectively. The metal concentrations were determined using a Spectro Ciros ICP-AE Spectrometer. A Photometer 7100 fully integrated with the Palintest water test system was used to measure ammonia over the ranges 0–1.0mg/l N. Dilutions were made using distilled water, depending on the original EC of each sample.

### Results and discussion

One of the most interesting results observed during the preparation of lime mixtures was the exothermic reaction of CaO to form  $\text{Ca}(\text{OH})_2$  immediately after the addition of the raw materials to distilled water, which was detected by a warming of the beaker containing the reaction mixture. As follows, we discuss the results corresponding to the characterization of the prepared mixtures by different analytical techniques and their application in the treatment of AMD through an adsorption batch experiment.

### X-ray diffraction analysis

X-ray patterns and assignments of the peaks of original kaolinite and metakaolinite and their synthesis products are presented in (Figure 1). It is evident that forming reactions of calcium silicate hydrates started very rapidly, after hydrothermal reaction of the starting materials in the system  $\text{CaO-SiO}_2\text{-Al}_2\text{O}_3\text{-H}_2\text{O}$ . Figure 1A shows that the characteristic reflection peaks of kaolinite (at 12.34° and 24.64° 2 $\theta$ ) decreased with reaction time.  $\text{Ca}(\text{OH})_2$  and C-S-H were the main phases identified at 0 h, along with relicts of kaolinite. The amount of

$\text{Ca}(\text{OH})_2$  increased with curing time and reached a maximum after 1h. Hydrogarnet and C-S-H were the reaction products formed after 1.5h of treatment, with the maximum and minimum amounts of hydrogarnet and C-S-H, respectively, after 24h. Hydrogarnet did not disappear after 24h of treatment, and the formation of tobermorite was observed after 2h and its amount increased gradually with reaction time. During the last stages of reaction,  $\alpha$ - $\text{C}_2\text{SH}$ , as reported by<sup>41</sup> and calcite also appeared. In Figure 1B the XRD patterns of metakaolinite and the resulting as-synthesized products after hydrothermal reaction with CaO solutions are illustrated. Metakaolinite showed a poor crystalline nature, with low-intensity peaks corresponding to quartz and muscovite, and was characterized by the appearance of an amorphous aluminosilicate (see the broad hump at  $2\theta=13\text{-}33^\circ$ ). According to Ríos et al.<sup>42</sup> this persists between 600 and 950°C, with relicts of the original kaolinite and mullite as the main crystalline phase at 1000°C. After metakaolinite/lime reaction, the most important hydrated phases were  $\text{Ca}(\text{OH})_2$ , hydrogarnet,  $\text{C}_2\text{ASH}_8$  and  $\text{C}_4\text{AH}_{13}$  at the early stages. Metastable phases like  $\text{C}_2\text{ASH}_8$  and  $\text{C}_4\text{AH}_{13}$  were also reported by Frias et al.<sup>24</sup> C-S-H,  $\alpha$ - $\text{C}_2\text{SH}$ , hydrogarnet and tobermorite were observed at the late stages. For comparison, a third mixture of pure chemical reagents (precipitated  $\text{SiO}_2$ ,  $\text{Al}_2\text{O}_3$  and CaO) was prepared and its as-synthesis products are illustrated in Figure 2.  $\text{Ca}(\text{OH})_2$ , C-S-H, katoite and calcite were the phases identified at 0 h, along with relicts of kaolinite. Reinik et al.<sup>43</sup> reported also the occurrence of katoite after hydrothermal alkaline treatment of oil shale ash. With curing time, katoite disappeared and new hydrated phases formed, which included C-S-H, hydrogarnet and tobermorite. It is evident that in the three investigated systems, hydrogarnet invariably appeared before 11Å tobermorite as reported in previous studies. Although the occurrence of metastable phases like  $\text{C}_2\text{ASH}_8$  and  $\text{C}_4\text{AH}_{13}$  is still unclear, we suggest that they were quickly converted to hydrogarnet, followed by tobermorite, with curing time. Le Saoût<sup>44</sup> reported the occurrence of the polymorphs of  $\text{CaCO}_3$  (calcite and aragonite), with calcite as the main crystalline material at the surface. Our XRD analysis did not detect it (except by traces of calcite in Figure 2 due to its very small crystal size, although the thermogravimetric analysis reveals the presence of  $\text{CaCO}_3$  as will be discussed later. The occurrence of  $\text{CaCO}_3$  can be explained by dissolution of carbon dioxide in the solution producing  $\text{CO}_3^{2-}$  ions, which react with  $\text{Ca}^{2+}$ ,<sup>44</sup> and the  $\text{Ca}^{2+}$  ions required by these reactions are obtained by the dissolution of C-H and by lowering the Ca/Si ratio of the C-S-H.<sup>45</sup>

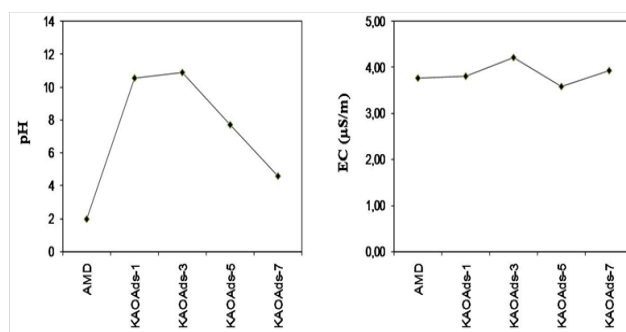


**Figure 1** Peaks of original kaolinite and metakaolinite and their synthesis products.

Several poorly crystalline materials, with un-reacted  $\text{Ca}(\text{OH})_2$  occurred at shorter reaction times. Hydrogarnet was always among the first phases formed and invariably appeared before 11Å tobermorite. However, later, with increasing reaction time, they started to fracture



and their quantity reduced almost in half over 24h. With increasing reaction time, hydrogarnet tended to undergo breakdown and its amount decreased and finally disappeared; CaO present in the further reaction with  $\text{SiO}_2$  formed hydrated calcium silicates, and released  $\text{Al}^{3+}$  ions were inserted into the Al-substituted tobermorite crystal lattice.<sup>27</sup> Different research groups have classified calcium silicate hydrates based on morphological and chemical data to compensate for scarce structural data. Taylor<sup>46</sup> classified C-S-H as C-S-H(I) and C-S-H(II) based on the Ca: Si ratio, with C-S-H(I) being obtained with Ca: Si < 1.5 and C-S-H(II) produced using Ca: Si > 1.5. Therefore, we consider that C-S-H(II) is the metastable phase that coexists with hydrogarnet and tobermorite, taking into account that we have used Ca: Si > 1.5 to prepare gel compositions, as precursors of the synthetic calcium silicate hydrate phases obtained in the present study.

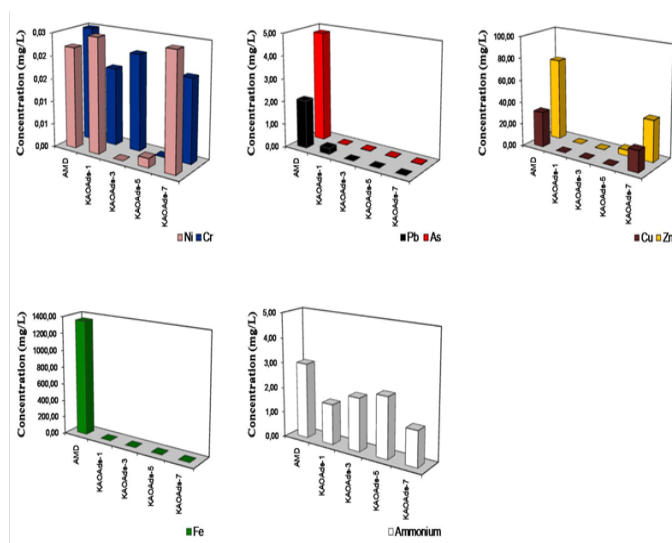


**Figure 2** For comparison, a third mixture of pure chemical reagents (precipitated  $\text{SiO}_2$ ,  $\text{Al}_2\text{O}_3$  and CaO) was prepared and its as-synthesis products.

### Scanning electron microscopy

SEM microphotographs of as-synthesized products autoclaved at  $175^\circ\text{C}$  for 0 and 24h. Synthesis products obtained from kaolinite/lime mixtures are characterized by the occurrence of flaky crystals of relict kaolinite associated with C-S-H and progressively with reaction time the breakdown of hydrogarnet, which in general shows an apparently intact surface. The typical octahedral morphology of hydrogarnet occurring in twinned crystals, developing clusters, obtained after metakaolinite/lime mixtures, whereas with reaction time tobermorite, showing typical Hebel microstructure, grew onto the hydrogarnet (rounded morphology) surface prior to its breakdown.

### Fourier transformed infrared spectroscopy

The structure of C-S-H gel is very complex. FT-IR has been found to be very useful in delineating the complex chemistry involved in the cement due to the poor crystallinity of silicate hydrates.<sup>47</sup> The FT-IR spectra in the region of  $1200\text{-}400\text{cm}^{-1}$  of the as-synthesized products from the investigated mixtures for kaolinite and metakaolinite for a mixture of precipitated  $\text{SiO}_2 + \text{Al}_2\text{O}_3$ , using CaO as activator. The broad bands centred at  $1115\text{-}1117\text{cm}^{-1}$  suggest the presence of C-S-H gels. This band decreased in intensity and exhibited a slight shift to lower frequencies with reaction time, and disappeared after

1.5h. Al-O stretching vibrations of tetrahedral  $\text{AlO}_4$  groups lie at  $1020\text{-}990\text{cm}^{-1}$ . The band at  $970\text{cm}^{-1}$  is attributed to Si-O stretching vibrations in C-S-H gels with jennite type structure.<sup>48</sup> The shoulder at  $914\text{-}918\text{cm}^{-1}$  may be assigned to OH bending vibrations in Al-OH-Al bonds (octahedral aluminium). The band appearing at  $798\text{-}800\text{cm}^{-1}$ , which is assigned to stretching vibrations modes of O-T-O groups (T=Al, Si), is attributed to polymerization and Si replacement by Al in tetrahedral sites of C-S-H. The bands of at  $873\text{-}879$  and  $696\text{-}700\text{cm}^{-1}$  can be attributed to calcite.

### Solid-state nuclear magnetic resonance

Hydration phases like calcium hydroxide (C-H) and calcium-silicate-hydrate (C-S-H) are closely linked, although C-H and C-S-H are considered as crystalline and nearly amorphous materials, respectively. Therefore, its structure must be studied by other methods and/or by analogy with natural or synthetic minerals such as zeolites. Some information on the structure of these compounds can be obtained by MAS-NMR.  $^{29}\text{Si}$  and  $^{27}\text{Al}$  NMR were performed on CaO-activated raw materials, revealing important information on the structure of the as-synthesized hydrated phases.

The  $^{29}\text{Si}$  and  $^{27}\text{Al}$  NMR spectra of kaolinite and its synthesis products. The  $^{29}\text{Si}$  NMR spectrum of kaolinite a single resonance centred at  $-91.4\text{ppm}$ , which is characteristic of layer silicates and assigned to Si linked via oxygens to three other Si atoms.<sup>49-50</sup> The chemical shift values of the  $^{29}\text{Si}$  NMR spectra of the treated kaolinite for 0 and 24h are indicating the occurrence of silicon sites of calcium silicate hydrate phases. A single resonance line at  $-91.3\text{ppm}$ , which can be attributed to the silicon site  $\text{Q}^3(1\text{Al})$  of  $\text{Ca}(\text{OH})_2$ , whereas three resonance lines at  $-79.5$ ,  $-85.3$  and  $-91.0\text{ppm}$ , which according to previous studies<sup>51-52</sup> can be assigned to the silicon sites  $\text{Q}^1$ ,  $\text{Q}^2(1\text{Al})$  and  $\text{Q}^3(1\text{Al})$  of C-S-H phases, respectively. The  $^{27}\text{Al}$  NMR spectrum of kaolinite consists of a single resonance at  $-3.4\text{ppm}$  that is assigned to 6-coordinated Al.  $^{27}\text{Al}$  NMR spectra of the treated kaolinite, with a single resonance at  $-3.7\text{ppm}$  attributed to 6-coordinated Al and three resonance lines at  $2.0$ ,  $11.6$  and  $55.4\text{ppm}$ ; the double peak (composed by the first two resonances) is assigned to 6-coordinated Al, while the last one is attributed to 4-coordinated Al.

The  $^{29}\text{Si}$  and  $^{27}\text{Al}$  NMR spectra of metakaolinite and its synthesis products. The  $^{29}\text{Si}$  NMR spectrum of metakaolinite displays a broad resonance in the chemical shift range from  $-75$  to  $-125\text{ppm}$ , centred at  $-96.3\text{ppm}$ , which can be assigned to the variety of silicon sites with Si linked to four other Si atoms in silica polymorphs<sup>53</sup> and indicates the presence of amorphous silica.<sup>41</sup> According to Mackenzie et al.<sup>54</sup> when kaolinite is dehydroxylated, the Si atoms undergo a range of environments of different distortion and the broadness of the metakaolinite line is attributed to these variations in the Si-O-Si(Al) bond angles. The chemical shift values of the  $^{29}\text{Si}$  NMR spectra of the treated metakaolinite for 0 and 24h respectively. A single resonance line at  $-91.2\text{ppm}$ , being attributed to the silicon site  $\text{Q}^3(1\text{Al})$  of  $\text{Ca}(\text{OH})_2$ , whereas two resonance lines at  $-79.4$  and  $-85.6\text{ppm}$  attributed to the silicon sites  $\text{Q}^1$  and  $\text{Q}^2(1\text{Al})$  of C-S-H phases. The  $^{27}\text{Al}$  NMR spectrum of metakaolinite displays two other resonances at  $-0.3\text{ppm}$  (assigned to 6-coordinated Al) and  $23.4\text{ppm}$  (attributed to 4-coordinated Al), which are, however, different compared with those reported by Rocha et al.<sup>49</sup> & Jiugao et al.<sup>50</sup> The broader and asymmetrical peak shapes of metakaolinite show its disordered structure.<sup>55</sup>  $^{27}\text{Al}$  NMR spectra of the treated metakaolinite show a single resonance at  $-1.9\text{ppm}$  attributed to 6-coordinated Al and three resonance lines at  $3.9$ ,  $11.7$  and  $55.6\text{ppm}$ ;

the double peak (composed by the first two resonances) is assigned to 6-coordinated Al, while the last one is attributed to 4-coordinated Al.

$^{29}\text{Si}$  NMR data reveal that silicon of the raw materials is completely converted with reaction time into C-S-H phases, including hydrogarnet and tobermorite. 11Å tobermorite exhibits two resonances at -85.7 and -95.7ppm attributed to chain middle group ( $\text{Q}^2$ ) and branching site ( $\text{Q}^3$ ).<sup>51</sup> We consider that the resonances at -85.3 and -85.6ppm can be assigned to 11Å tobermorite. However, the lack of the resonance at -95.7ppm reported by Wieker et al.<sup>51</sup> can be explained by an overlapping of resonances corresponding to different calcium silicate hydrates. Komarneri et al.<sup>52</sup> showed that the substitution of aluminium in tobermorite caused a low field shift of the  $\text{Q}^3$  units from -95.7 to -91.5ppm, which can also explain the occurrence of the resonance at -91.0ppm. According to, whereas  $^{27}\text{Al}$  NMR data indicate the appearance of tobermorite at longer reaction time (24h), although it is difficult to suggest the occurrence of Al-substituted tobermorite or other Al-substituted C-S-H phase, as has been reported by other studies.<sup>52-56</sup>

### Thermogravimetric analysis (TGA)

Thermogravimetry (TG) and derivative thermogravimetry (DTG) have proven to be valuable tools for evaluating the nature of hydration products according to different stages of cement hydration, as well as quantifying the different phases.<sup>57-61</sup> The identity of the amount of the hydrated phases was estimated from thermogravimetric analysis. Hydration products, mainly calcium silicate hydrates (C-S-H gel) and portlandite ( $\text{Ca}(\text{OH})_2$ ), are the result of hydration of the main components of cement. The hydration rate of cement can be evaluated by measuring the mass loss of hydrated compounds  $\leq 700^\circ\text{C}$ . Different DTG peaks or temperature ranges were obtained when the C-S-H gel was heated between 25 and  $700^\circ\text{C}$ :  $100^\circ\text{C}$ , dehydration of pore water;  $100\text{-}250^\circ\text{C}$ , different stages of C-S-H dehydration;  $\sim 250\text{-}350^\circ\text{C}$ , presence of a member of the hydrogarnet group;  $\sim 350\text{-}500^\circ\text{C}$ , decomposition of  $\text{Ca}(\text{OH})_2$ ;  $\sim 500^\circ\text{C}$ , dehydroxylation of  $\text{Ca}(\text{OH})_2$ ;  $\sim 573^\circ\text{C}$ : crystalline inversion of quartz;  $\sim 700^\circ\text{C}$ , decarbonation of  $\text{CaCO}_3$ . A large amount of water is released between 100 and  $250^\circ\text{C}$  when the C-S-H gel began to decompose. According to Klimesch et al.<sup>22</sup> hydrogarnet amount increased slightly up to 2h, followed by a decrease clearly demonstrating that this phase was decomposed and consumed with reaction time. C-S-H formation was enhanced with the use of the metakaolinite/lime mixture as indicated by the size and presence of several endotherms, compared with the other two mixtures, which indicates that the  $\text{SiO}_2$  source originating from metakaolinite is more reactivity than that from precipitated  $\text{SiO}_2$  and kaolinite.

Tobermorite appeared after 2h of autoclaving and increased with reaction time. However, the addition of metakaolinite to the mixture promoted a decrease in tobermorite formation. A weight loss of 23.36, 27.06 and 22.70% was obtained when kaolinite, metakaolinite and precipitated  $\text{SiO}_2 + \text{Al}_2\text{O}_3$ , respectively, were activated with CaO. The metakaolinite/lime mixture produced the highest weight loss, which indicates that this mixture had high water contents. However, it should be noted that the weight loss is overlapped by calcium silicate hydrates, which are known to dehydrate gradually and differently over a wide temperature range  $\leq 800^\circ\text{C}$ .<sup>62</sup> Differences in their dehydration behaviour are due to compositional and structural variations.<sup>63</sup>

In general, the results of the thermogravimetric analysis indicates that the addition of CaO to kaolinite and metakaolinite produced

several water containing phases in the temperature range  $25\text{-}350^\circ\text{C}$ . On the other hand, the DTA curves show the decomposition of portlandite (at  $\sim 440^\circ\text{C}$ ) and calcite (at  $\sim 680^\circ\text{C}$ ). Two interesting aspects observed are: a crystalline inversion of quartz (peak at  $551^\circ\text{C}$ ) and the presence of  $\text{C}_2\text{ASH}_8$  and  $\text{C}_4\text{AH}_{13}$ , as reported by Frias et al.<sup>24</sup>

### AMD treatment using kaolinite-based calcium silicate hydrates

The surface drainage waters at Parys Mountain are strongly acidic ( $\text{pH} < 2$ ) and metal-rich due to the oxidation of sulphide minerals, and its orange-brown colour is due to the very high concentrations of ferric iron in solution. Neutralization is generally the first step in treating AMD. The neutralization reaction of AMD was examined measuring the pH and electrical conductivity of sorbent: AMD mixtures (0.25g/20ml) over a period of 30 minute. pH and electrical conductivity trends obtained after treatment of AMD. KAOAds-3 produced the highest pH (10.87), whereas using KAOAds-7 as an adsorbent, the lowest pH (4.55) was obtained, which indicates that the sample KAOAds-3 showed the best neutralization capacity, due to the presence of portlandite as the main calcium silicate hydrate phase. However, pH increased as a consequence of the progressive dissolution of the sorbent (kaolinite-based calcium silicate hydrates) during the shaking process. The electrical conductivity of the treated AMDs did not show strong fluctuations or changes compared with raw AMD.

The removal of metal ions (Cu, Pb, Zn, Ni, Cr, As and Fe) and ammonium from AMD using kaolinite-based calcium silicate hydrates for a sorbent: AMD mixture of 0.25g/20ml. The removal trends of metal ions in the final leachates for the investigated mixtures are described as follows. Cu was almost completely removed using all samples, except KAOAds-7, which produced the higher Cu concentration (19.17ppm), whereas KAOAds-1 (portlandite) produced the lower residual concentration of Cu (0.029ppm). Pb shows a reversal behaviour compared with that observed for Cu, with a progressive decrease of concentration with curing time, which means that KAOAds-1, containing a single phase (portlandite) had a lower efficiency in Pb removal compared with KAOAds-7, which is composed of several calcium silicate hydrate phases like hydrogarnet and tobermorite. Zn displayed similar behaviour to that observed for Cu, although the highest residual concentration (37.230ppm) was obtained using KAOAds-7. Ni, Cr and as did not show consistent trends, which is evident from the slight fluctuations. The addition of the mixtures KAOAds-3 and KAOAds-5, which are characterized by the occurrence of several calcium silicate hydrates, except tobermorite, produce higher concentrations of Fe compared with those obtained using portlandite (KAOAds-1) and KAOAds-7. The final ammonium concentration obtained for the same mixtures. The samples KAOAds-1 and KAOAds-7 produced the lower residual concentration values, particularly the second one that contains tobermorite, whereas the higher concentration of ammonium was obtained after addition of KAOAds-5, which contains various calcium silicate hydrates (except tobermorite). Preliminary results demonstrate that the kaolinite-based calcium silicate hydrates can be used for remediation of AMD by removing heavy metals and ammonium.

### Concluding remarks

Different C-S-H materials were synthesized in the system  $\text{CaO-SiO}_2\text{-Al}_2\text{O}_3\text{-H}_2\text{O}$  under hydrothermal conditions at  $175^\circ\text{C}$  for a

monitoring time of 24h. The morphological, chemical and structural data determined by several analytical techniques are consistent and show good agreement with the literature. Some of the advantages to use an  $\text{Al}_2\text{O}_3$  source such as kaolinite or metakaolinite is that Al accelerates tobermorite formation from C-S-H, inhibits the conversion to xonotlite, which reduces the strength properties of the synthetic product, and extends the temperature range over which tobermorite is stable.<sup>64</sup> Metakaolinite is a more reactive phase than kaolinite for release of Al to form Al-tobermorite.

Several poorly crystalline materials occurred with un-reacted  $\text{Ca}(\text{OH})_2$  at shorter reaction times. Hydrogarnet and tobermorite are interesting phases formed in the treated samples at longer curing times, which should promote the strength development of the synthesis products. Hydrogarnet was always among the first phases formed and invariably appeared before 11Å tobermorite. However, later, with increasing reaction time, they start to fracture and their quantity reduced almost in half during 24h.

Our results indicate that hydrogarnet is always one of the first phases formed. However, its continued existence in the final product depends on factors, such as reaction time and bulk composition. In the subsequent autoclaving process the reaction continues and tobermorite is formed, which is known to provide hardness and strength to the final material.

The thermal stability of the as-synthesized pastes shows the process of dehydration of free water and decomposition of the C-S-H gel from 25 to 250°C. The weight losses between 400 and 500°C are due to the decomposition of portlandite. The decomposition of carbonate phases occurred at ~ 500°C.

It is well known that calcium silicate hydrates exhibit a good capability to fix metals and metalloids. Tobermorite is a calcium silicate hydrate substituted with  $\text{Al}^{3+}$  and alkali, which exhibits cation exchange and selectivity properties for Cs and Rb, falling between those of clay minerals and zeolites. Unlike clay minerals and zeolites, tobermorite is expected to be thermodynamically stable in cement and concrete which have a similar chemical composition and therefore, it will be suitable for inexpensive solidification in cement after their use in the decontamination of radioactive species from nuclear wastes. Therefore the capabilities of those phases to retain heavy metals should be evaluated. A batch sorption study confirmed that the C-S-H-bearing products were effective in the exclusion of metal ions and ammonium from AMD. The as-synthesized C-S-Hs could be recognized as materials with potential applications in heavy metal removal from polluted effluents. However, in spite of their cation exchange capacity represents a very important characteristic quality in the removal of undesired species from aqueous solutions, it is not the deciding factor affecting the performance this cation exchanger during ion exchange processes, since numerous other factors also need to be considered.

## Acknowledgements

The first author would like to thank the Programme AlBan, the European Union Programme of High Level Scholarships for Latin America (scholarship no. E05D060429CO), and the Universidad Industrial de Santander (remunerated commission). This research has benefited from research facilities provided by the School of Applied Sciences at the University of Wolverhampton.

## Conflict of interest

The author declares no conflict of interest.

## References

- Bonaccorsi E, Merlino S. *Calcium silicate hydrate (C-S-H) minerals: structures and transformations*. 32 International Geological Congress. Firenze, 2004. 215 p.
- Sakiyama M, Mitsuda T. Hydrothermal reaction between C-S-H and kaolinite for the formation of tobermorite at 180°C. *Cem Concr Res*. 1977;7:681–686.
- Mitsuda T, Taylor HFW. Influence of aluminium on the conversion of calcium silicate hydrate gels into 11Å tobermorite at 90°C and 120°C. *Cem Concr Res*. 1979;5:203–209.
- Komarneni S, Roy DM. Tobermorites a new family of cation exchangers. *Science*. 1983;221:647–648.
- Shrivastava OP, Shrivastava R. Study of selective sorption of Cs-137 on Al-substituted calcium silicate hydroxyl hydrate. *J Indian Chem Soc*. 2001;78(8):392–394.
- El-Hemaly SAS, Mitsuda T, Taylor HFW. Synthesis of normal and anomalous tobermorites. *Cem Concr Res*. 1977;7:429–438.
- Siaucinas R, Sasnauskas K, Balandis A. Investigations of synthesis processes of calcium silicate hydrates of low basicity with participation of aluminium. *Chemine Technol*. 1999;11:31–38.
- Sridhar Komarneni, Della M Roy. New tobermorite cation exchangers. *Journal of Materials Science*. 1985;20:2923–2936.
- Chikashi Tamura, Zhidong Ya, Fumio Kusano, et al. Conversion of waste incineration fly ash into Al-substituted tobermorite by hydrothermal treatment. *Journal of the Ceramic Society of Japan*. 2000;108:150–155.
- Coleman NJ. Synthesis, structure and ion exchange properties of 11Å tobermorites from newsprint recycling residue. *Mater Res Bull*. 2005;40:2000–2013.
- Abo-El-Einen SA, Gabr NA, Mikhail R Sh. Morphology and microstructure of autoclaved clinker and slag-lime pastes in presence and absence of silica sand. *Cem Concr Res*. 1977;7:231–238.
- Abo-El-Einen SA, Gabr NA, Mikhail RSh. Morphology and microstructure of autoclaved slag-clinker pastes in presence and absence of silica sand. *Cem Concr Res*. 1977;7:363–368.
- Kalousek GL. Crystal chemistry of hydrous calcium silicates: I, substitution of aluminum in lattice of tobermorite. *Journal of American Ceramic Societ*. 1979;40:74–80.
- Van Aardt JHP, Visser S. Reaction of  $\text{Ca}(\text{OH})_2$  and of  $\text{Ca}(\text{OH})_2 + \text{CaSO}_4 \cdot 2\text{H}_2\text{O}$  at various temperatures with feldspars in aggregates used for concrete making. *Cem Concr Res*. 1978;8:677–681.
- Serry MA, Taha AS, El-Hemaly H. El-Didamony, Metakaolin-lime hydration products. *Thermochim Acta*. 1984;79:103–110.
- Atkins M, Macphee D, Kindness A, et al. Solubility properties of ternary and quaternary compounds in the  $\text{CaO-Al}_2\text{O}_3\text{-SO}_3\text{-H}_2\text{O}$  system. *Cem Concr Res*. 1991;21:991–998.
- Al-Wakeel EI, El-Korashy SA. Reaction mechanism of the hydrothermally treated  $\text{CaO-SiO}_2\text{-Al}_2\text{O}_3$  and  $\text{CaO-SiO}_2\text{-Al}_2\text{O}_3\text{-CaSO}_4$  systems. *J Mater Sci*. 1996;31:1909–1913.
- Afridia MUK, Ohamab Y, Demurab K, et al. Hydrogarnet-type cubic crystals in polymer-modified mortars. *Cem Concr Res*. 1997;27:1787–1789.
- Jie Wang, Akira Tomita. Hydrothermal Reaction of Kaolinite with Calcium Hydroxide and Dissolution of Reaction Products in Hydrochloric Acid. *Ind Eng Chem Res*. 1997;36:5258–5264.



20. Klimesch DS, Ray A. Hydrogarnet formation during autoclaving at 180°C in unstirred metakaolin–lime–quartz slurries. *Cem Concr Res.* 1998;28:1109–1117.
21. Klimesch DS, Ray A. Effects of quartz particle size on hydrogarnet formation during autoclaving at 180°C in the  $\text{CaO-Al}_2\text{O}_3\text{-SiO}_2\text{-H}_2\text{O}$  system. *Cem Concr Res.* 1998;28:1309–1316.
22. Klimesch DS, Ray A. DTA–TGA of unstirred autoclaved metakaolin–lime–quartz slurries. The formation of hydrogarnet. *Thermochimica Acta.* 1998;316(2):149–154.
23. Klimesch DS, Ray A. Effects of quartz particle size and kaolin on hydrogarnet formation during autoclaving. *Cement And Concrete Research.* 1998;28:1317–1323.
24. Frías M, Cabrera J. The effect of temperature on the hydration rate and stability of the hydration phases of metakaolin–lime–water systems. *Cem Concr Res.* 2002;32:133–138.
25. NJ Coleman, DS Brassington. Synthesis of Al–substituted 11Å tobermorite from newsprint recycling residue: a feasibility study. *Mat Res Bull.* 2003;38:485–497.
26. Frías M, Sánchez MI. The effect of high curing temperature on the reaction kinetics in MK/lime and MK–blended cement matrices at 60°C. *Cement and Concrete Research.* 2003;33:643–649.
27. Siauciunas R, Baltusnikas A. Influence of  $\text{SiO}_2$  modification on hydrogarnets formation during hydrothermal synthesis. *Cem Concr Res.* 2003;33:1789–1793.
28. Frías M, Moisés, Sánchez de Rojas, et al. Influence of metastable hydrated phases on the pore size distribution and degree of hydration of MK–blended cements cured at 60°C. *Cem Concr Res.* 2005;35:1292–1298.
29. Rujiwatra A, Phueadpho M, Grudpan K. Selective synthesis of zeolitic phillipsite and hibschite hydrogarnet from lignite ash employing calcium hydroxide under mild conditions. *J Phys Chem Solids.* 2005;66:1085–1090.
30. Rose J, Bénard A, El Mrabet S, et al. Evolution of iron speciation during hydration of  $\text{C}_4\text{AF}$ . *Waste Manag.* 2006;26:720–724.
31. Sarkar R, Das SK, Mandal PK, et al. Phase and microstructure evolution during hydrothermal solidification of clay–quartz mixture with marble dust source of reactive lime. *J Eur Ceram Soc.* 2006;26:297–304.
32. Frías M. Study of hydrated phases present in a MK–lime system cured at 60°C and 60 months of reaction. *Cem Concr Res.* 2006;36:827–831.
33. Rivas JM, Pena P, De Aza, et al. Solid–state  $^{27}\text{Al}$  and  $^{29}\text{Si}$  NMR investigations on Si–substituted hydrogarnets. *Acta Mater.* 2007;55:1183–1191.
34. Klimesch DS, Lee G, Ray A, et al. Metakaolin additions in autoclaved cement–quartz pastes: A  $^{29}\text{Si}$  and  $^{27}\text{Al}$  MAS NMR investigation. *Advances in Cement Research.* 1998;10:93–99.
35. Komarneni S, Roy DM, Roy R. Al–substituted tobermorite: shows cation exchange. *Cem Concr Res.* 1982;12:773–780.
36. Sridhar Komarneni, Della M Roy. New tobermorite cation exchangers. *Journal of Materials Science.* 1985;20(8):2930–2936.
37. Nitin Labhasetwar, Shrivastava OP. Ion–exchange properties of 11–Å tobermorite. *React Solids.* 1986;2:261–268.
38. Labhasetwar N, Shrivastava OP.  $\text{Ca}^{2+} \rightleftharpoons \text{Pb}^{2+}$  exchange reaction of calcium silicate hydrate:  $\text{Ca}_5\text{Si}_6\text{O}_{18}\text{H}_2\cdot 4\text{H}_2\text{O}$ . *Journal of Materials Science.* 1989;24:4359–4362.
39. Shrivastava OP, Shrivastava R.  $\text{Sr}^{2+}$  uptake and leachability study on cured aluminum–substituted tobermorite–OPC admixtures. *Cement And Concrete Research.* 2001;31:1251–1255.
40. Komarneni S, Komarneni JS, Newalkar B, et al. Microwave–hydrothermal synthesis of Al–substituted tobermorite from zeolites. *Mater Res Bull.* 2002;37:1025–1032.
41. Hartmann A, Buhl J Ch, Van Breugel K. Structure and phase investigations on crystallization of 11Å tobermorite in lime sand pellets. *Cem Concr Res.* 2007;37:21–31.
42. Ríos CA, Williams CD, Maple MJ. Synthesis of zeolites and zeotypes by hydrothermal transformation of kaolinite and metakaolinite. *Bistua.* 2007;5:15–26.
43. Reinik J, Heinmaa I, Mikkola JP, et al. Hydrothermal alkaline treatment of oil shale ash for synthesis of tobermorites. *Fuel.* 2007;86:669–676.
44. Le Saoût G, Lécolier E, Rivereau A, et al. Chemical structure of cement aged at normal and elevated temperatures and pressures, Part II: Low permeability class G oilwell cement. *Cem Concr Res.* 2006;36:428–433.
45. Taylor HFW. *Cement Chemistry.* 2nd ed. London: Thomas Telford Publishing; 1997.
46. Taylor HFW. *Cement Chemistry.* London: Academic Press Ltd; 1990.
47. Yu P, Kirckpatrick RJ, Poe B, et al. Structure of calcium silicate hydrate (C–S–H): near–, mid–, and far–infrared spectroscopy. *J Am Ceram Soc.* 1999;82:742–748.
48. Hidalgo A, Petit S, Domingo C, et al. Microstructural characterization of leaching effects in cement pastes due to neutralisation of their alkaline nature. Part I: Portland cement pastes. *Cement and Concrete Research.* 2007;37:63–70.
49. Rocha J, Klinowski J.  $^{29}\text{Si}$  and  $^{27}\text{Al}$  magic–angle–spinning NMR studies of the thermal transformation of kaolinite. *Physics and Chemistry of Minerals.* 1990;17:179–186.
50. Jiugao G, Fuya W, Fuya W. Kaolinite–mullite reaction series: A  $^{27}\text{Al}$  and  $^{29}\text{Si}$  MAS NMR study. *Acta Miner Sinica.* 1997;17:250–259.
51. Wieker W, Grimmer AR, Winkler A, et al. Solid–state high–resolution  $^{29}\text{Si}$  NMR spectroscopy of synthetic 14Å, 11Å and 9Å tobermorites. *Cem Concr Res.* 1982;12:333–339.
52. Komarneni S, Roy R, Roy DM, et al.  $^{27}\text{Al}$  and  $^{29}\text{Si}$  magic angle spinning nuclear magnetic resonance spectroscopy of Al–substituted tobermorites. *J Mater Sci.* 1985;20:4209–4214.
53. Smith JV, Blackwell CS. Nuclear magnetic resonance of silica polymorphs. *Nature.* 1983;303:223–225.
54. Mackenzie KJD, Brown IWM, Meinhold RH, et al. Outstanding problems in the kaolinite–mullite reaction sequence investigated by  $^{29}\text{Si}$  and  $^{27}\text{Al}$  Solid–State Nuclear Magnetic Resonance: I. Metakaolinite. *J Am Ceram Soc.* 1985;68:293–297.
55. Liu Q, Spears DA, Liu Q. MAS NMR study of surface–modified calcined kaolin. *Appl Clay Sci.* 2001;19:89–94.
56. Faucon P, Charpentier T, Nonat A, et al. Triple–quantum two dimensional  $^{27}\text{Al}$  magic angle nuclear magnetic resonance study of aluminum incorporation in calcium silicate hydrates. *J Am Chem Soc.* 1998;120:75–82.
57. Fordham CJ, Smalley IJ. A simple thermogravimetric study of hydrated cement. *Cem Concr Res.* 1985;15:141–144.
58. Chandra S, Flodin P. Interactions of polymers and organic admixtures on portland cement hydration. *Cement and Concrete Research.* 1990;17:975–990.
59. Ollitrault–Fichet R, Gauthier C, Clamen G, et al. Microstructural aspects in a polymer–modified cement. *Cem Concr Res.* 1998;28:1687–1693.
60. Tisivilis S, Kakali G, Chaniotakis E, et al. A study on the hydration of Portland limestone cement by means of TG. *Journal of Thermal Analysis and Calorimetry.* 1998;52:863–870.
61. Dweck J, Buchler P, Coelho A, et al. Hydration of a Portland cement blended with calcium carbonate. *Thermochim Acta.* 2000;346:105–113.
62. Okada Y, Sasaki K, Zhong B, et al. Formation processes of  $\beta\text{-C}_2\text{S}$  by the decomposition of hydrothermally prepared C–S–H with  $\text{Ca}(\text{OH})_2$ . *J Am Ceram Soc.* 1994;77:1319–1324.
63. Pushnyakova VA, Kotsupalo NP, Berger AS. *J Appl Chem.* 1975:481497.
64. Larosa–Thompson JL, Grutzeck MW. C–S–H, tobermorite, and coexisting phases in the system  $\text{CaO-Al}_2\text{O}_3\text{-SiO}_2\text{-H}_2\text{O}$ . *World Cem.* 1996:169–74.